Journal of Renewable Materials

Tech Science Press

DOI: 10.32604/jrm.2022.023214

ARTICLE

A Primary Study on Mechanical Properties of Heat-Treated Wood via *in-situ* Synthesis of Calcium Carbonate

Dianen Liang[1], Zhenhao Ding[1], Qilin Yan[1], Redžo Hasanagić[2], Leila Fathi[3], Zi Yang[1], Longhao Li[1], Jianbo Wang[1], Houhua Luo[1], Qian Wang[1] and Demiao Chu[1,*]

[1]Key Lab of State Forest and Grassland Administration on "Wood Quality Improvement & High Efficient Utilization", School of Forestry & Landscape Architecture, Anhui Agricultural University, Hefei, China

[2]Department of Wood Science and Technology, Faculty of Technical Engineering, University of Bihać, Bihać, Bosnia and Herzegovina

[3]Department of Natural Resources and Earth Science, Shahrekord University, Shahrekord, Iran

[*]Corresponding Author: Demiao Chu. Email: Demiaochu@ahau.edu.cn

Received: 15 April 2022 Accepted: 26 May 2022

ABSTRACT

This study aims to improve the value of fast-growing wood and extend the heat-treated wood utilization using inorganic calcium carbonate ($CaCO_3$) crystals via an *in-situ* synthesis method. $CaCl_2$ and Na_2CO_3 solutions with a concentration ratio of 1:1 were successively introduced into the thermally modified poplar wood obtained by steam heat treatment (HT) at 200°C for 1.5 and 3 h, resulting in the *in-situ* synthesis of $CaCO_3$ crystals inside the heat-treated wood. The filling effect was best at the concentration of 1.2 mol/L. $CaCO_3$ was uniformly distributed in the cell cavities of the heat-treated wood, and some of the crystals were embedded in the fissures of the wood cell walls. The morphology of $CaCO_3$ crystals was mainly spherical and rhombic polyhedral. Three main types of $CaCO_3$ crystals were calcite, vaterite, and aragonite. The HT of poplar wood at 200°C resulted in degrading the chemical components of the wood cell wall. This degradation led to reduced wood mechanical properties, including the surface hardness (HD), modulus of rupture (MOR), and modulus of elasticity (MOE). After $CaCO_3$ was *in-situ* synthesized in the heat-treated wood, the HD increased by 18.36% and 16.35%, and MOR increased by 14.64% and 8.89%, respectively. Because of the $CaCO_3$ synthesization, the char residue of the 200°C heat-treated wood samples increased by 9.31% and the maximum weight loss rate decreased by 19.80%, indicating that the filling with $CaCO_3$ cannot only improve the mechanical properties of the heat-treated wood but also effectively enhance its thermal stability.

KEYWORDS

Heat treatment; poplar wood; calcium carbonate; *in-situ* synthesis; reinforcement

1 Introduction

In order to promote the construction of ecological civilization and protect the ecological environment, China bans all commercial harvesting of wild forest timber. China has abundant plantation wood resources; China's plantation forest area ranks first in the world [1]. Unfortunately, the fast growing of wood have some negative effects on its quality, including density, dimensional stability and mechanical strength. Therefore,

the efficient utilization of the fast-growing wood is a critical problem that requires a remedy in the timber industry.

Various organic and inorganic wood modification methods have been developed to address the efficient utilization of fast-growing wood [2]. The three main commercialized wood modification processes (acetylation, furfurylation, heat treatment) have gradually gained a foothold in European companies [3]. Acetylation implies impregnation with acetic anhydride followed by substitution of the hydroxyl group with acetyl groups [4]. Not only does the the acetylation process improves the dimensional stability and durability of the wood cells, but it also insignificantly affects the wood strength [5]. Furfurylation is an impregnation process with furfuryl alcohol that produces furan polymers within the cell walls of the wood. Furfurylation renders cell walls swollen, thereby reducing the moisture absorption of the wood and improving its dimensional stability and decay resistance. Compared to these methods, HT is generally considered more environmentally friendly as no chemical modification reagents are involved during the process [6].

Heat treatment (HT) is an environmentally friendly wood modification approach that can improve many performance deficiencies of fast-growing forest wood, such as dimensional stability and durability, but often at the cost of reducing the mechanical strength of the wood [7–9]. Further studies on heat-treated wood at elevated temperatures have shown that high temperatures render wood brittle. The brittle surface layer results in forming smaller sawdust particles during wood machining. Moreover, the surface roughness increases significantly after processing, and the mechanical properties of the wood surface of the cell wall decrease due to high-temperature thermal degradation [10]. Another study revealed HT changes the crystal structure of the rigid skeleton of wood and causes brittle changes, making the wood less resistant to damage when subjected to bending, tensile, and impact loads [11]. Besides, the chemical degradation during the high-temperature HT process does not improve the thermal stability of wood [12].

There is an increasing interest in applying natural and eco-friendly materials in wood modification technology [13,14]. $CaCO_3$ is an efficient and cost-effective fire-retardant filler with low solubility, high whiteness, high strength, and satisfactory thermal stability. $CaCO_3$ modifies cellulose and improves the hardness, thermal stability, and friction properties of the wood [15,16]. Merk et al. [17] studied the mineralisation of the wood cell wall architecture with $CaCO_3$ and found that it effectively improved the flame retardancy and reliability of unmodified wood; Rožle et al. [18] studied a combination of the thermal modification followed by the mineralisation process, and found that $CaCO_3$ mineralization treatment improved the durability of thermally modified wood. Moreover, some studies also proved that some organic modified formulations may produce toxic substances in use, recycling or even fires, and that $CaCO_3$ fillers have environmental advantages over them [19–23]. The widespread use of phosphorous flame retardant containing organophosphate esters, for instance, poses some environmental hazards [24]. However, as far as we know, there is a research gap on how $CaCO_3$ could improve heat-treated wood.

Therefore, $CaCO_3$ was *in-situ* synthesized in the thin heat-treated poplar wood board by immersing in $CaCl_2$ and Na_2CO_3 solutions under vacuum conditions in the present study. Optimum impregnating solutions at different concentration levels were used to improve the effectiveness of HT on the mechanical properties of poplar wood. The thermal stability of the heat-treated wood is also improved since the suppression of wood mass loss is the basis for the structure and strength of wood [25]. This study attempts to investigate efficiency of precursor solutions on the *in-situ* synthesis weight percent gain and the effects of $CaCO_3$ on the mechanical properties, and thermal stability of combine-modified poplar wood. In addition, this study aims to provide an innovative method for *in-situ* reinforcement modification of heat-treated poplar wood with brittle cell walls, boosting the utilization of the HT technology.

2 Materials and Methods

2.1 Materials

Ten of the 12-year-old Populus (Zhonglin 46 Populus) were procured from Nongcui Garden of Anhui Agricultural University, Hefei, China. They were sawed into 200 mm × 150 mm × 30 mm (length × width × thickness) and air-dried. Then, the timbers were cut to the dimensions of 100 mm × 20 mm × 5 mm (length × width × thickness). All the samples were defect-free and flat-sawn. Calcium chloride ($CaCl_2$) and sodium carbonate (Na_2CO_3) were analytically pure purchased from Sinopharm Chemical Reagent Co., Ltd. (China).

2.2 Thermal Treatment Process and Preparation of Modified Wood Samples

Using the water vapor protection method, a self-made high-temperature test box was used to conduct high-temperature HT on the poplar wood, and the cistern is installed as a steam generating device [26]. The modification process and treatment levels are shown in Fig. 1 and Table 1.

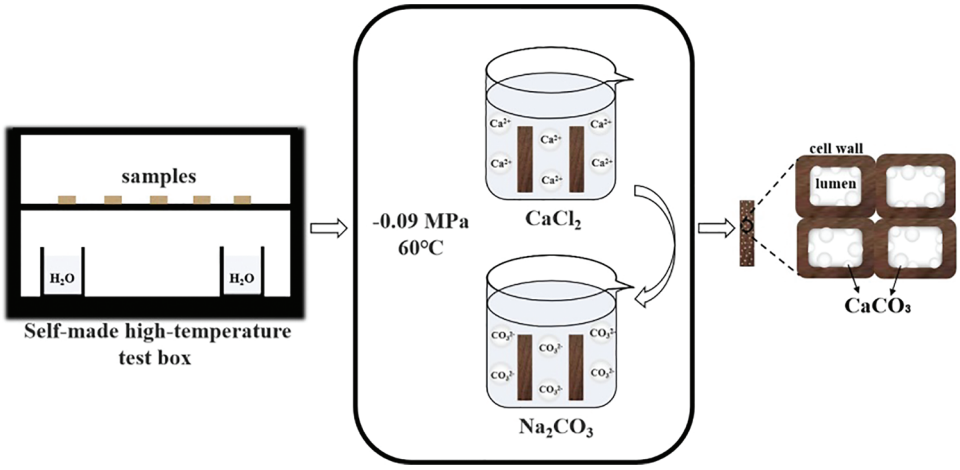

Figure 1: Schematic illustration of the preparation of modified wood

Table 1: Treatment levels of the modified wood samples

Treatment level	Heat treatment (HT)		Impregnation
	Heat (200°C)	Duration (h)	
UT	NO	NO	NO
CI	NO	NO	YES
HT-1.5	YES	1.5	NO
HT-3	YES	3	NO
CI-HT-1.5	YES	1.5	YES
CI-HT-3	YES	3	YES

The $CaCl_2$ solution and Na_2CO_3 solution were used to prepare the $CaCO_3$ modified wood samples. First, untreated and heat-treated samples were impregnated in the concentration of 0.4, 0.8, 1.2, 1.6, 2.0 mol/L $CaCl_2$ solution in a vacuum drying oven at a temperature of 60°C and vacuum decompression filtration for 4 times, then maintained −0.09 MPa for 4 h. After the impregnation process of $CaCl_2$ solution, the

samples were oven-dried at a temperature of 60°C for 6 h. Next, the same impregnation process using Na_2CO_3 solution was conducted. The optimized solution concentration will be selected for further study based on the investigation of impregnation efficiency, here we found is 1.2 mol/L.

2.3 Physical and Mechanical Properties Tests

Twelve specimens in each groups were oven dried at 103°C to a constant weight and the weight gain (WPG, %) of wood specimens after *in-situ* synthesis by $CaCO_3$ were calculated as:

$$\mathrm{WPG} = \frac{M_1 - M_0}{M_0} \times 100\% \tag{1}$$

where M_0(g) is the absolute dry mass of the specimen before impregnation treatment, and M_1(g) is the absolute dry mass of the specimen after impregnation treatment.

Before conducting mechanical properties testing, fifteen specimens in each group were subjected to humidification balance treatment in a conditioning chamber with a temperature of 20°C and relative humidity of 65%. The surface Shore D hardness (HD) test was carried out using a TH210 Shore hardness tester. A high precision double column universal mechanical testing machine (AG-X plus, Shimadzu, Japan) with a load cell of 5 kN was employed to measure the modulus of rupture (MOR) and modulus of elasticity (MOE) of the samples. According to GB/T 17657–2013, the three-point bending test was applied, the span of the samples is 50 mm, and indenter drop speed is 5 mm/min [27].

2.4 Characterization and Analysis

A high-speed universal pulverizer (FW-100, Beijing Zhongxing Weiye Instrument Co., Ltd., China) was employed to prepare wood powder samples. Next, thermal stability tests were accomplished using a thermogravimetric analyzer (TG 209F3, NETZSCH, Germany). For this test, three replicates of 4–6 mg wood powder underwent 60 ml/min nitrogen flow rate test conditions from room temperature (23°C) to 700°C with a heating rate of 15 K/min. The TG and DTG curves were obtained by processing the calculated data using origin.

Hierarchical cluster analysis (HCA) was performed using IBM SPSS Statistics 22.0 by the between-group linkage method [28] The values of the surface hardness (HD), the modulus of rupture (MOR), and modulus of elasticity (MOE) were taken into consideration, respectively.

Fourier transform infrared (FTIR) spectroscopy was carried out on an FTIR spectrometer (TENSOR II, BRUKER, Germany) with a wavenumber range from 4000 to 400 cm^{-1}, resolution of 8 cm^{-1}, and a frequency of 32 times.

X-ray diffraction (XRD) analysis (XD6, PERSEE, China) was employed with Cu Ka radiation (0.15406 nm) and a measurement range of 10°–80°. Segal's empirical method was used to calculate the crystallinity of the wood cellulose [29].

Scanning electron microscopy (SEM Sirion 200, FEI, USA) was used to analyze the grain morphology of the *in-situ* synthesized $CaCO_3$. All samples were Au coated prior to examination.

2.5 Statistical Analyses

Differences between samples were tested for significance by the Tukey honest significance test using origin for the values of the surface hardness (HD), the modulus of rupture (MOR), and modulus of elasticity (MOE).

3 Results and Discussion

3.1 The Influence of the Impregnation Solution Concentration on Weight Percent Gain

Fig. 2 shows the weight gain (WPG, %) of the modified samples at different treatment levels (different impregnating solution concentration levels). The WPG of CI, CI-HT-1.5, and CI-HT-3 elevated as the impregnating solution concentration increased.

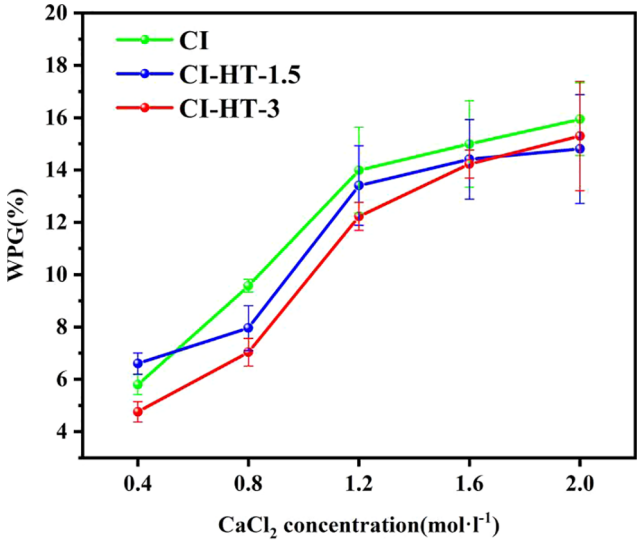

Figure 2: The weight percent gain of the modified woods under different concentrations

Different impregnation solution concentrations significantly affected the synthesis of $CaCO_3$ in poplar wood [30]. When the impregnating solution concentration was 0.4 mol/L, the weight gain value was relatively low, the WPG of CI, CI-HT-1.5, and CI-HT-3 was 5.79%, 6.60%, and 4.76%, respectively. When the impregnating solution concentration is 0.4 mol/L, WPG showed a nonlinear increase trend with the increase of the impregnating solution concentration. The WPG of CI, CI-HT-1.5, and CI-HT-3 all reached the maximum value at the impregnating solution concentration of 2.0 mol/L with 15.94%, 14.80%, and 15.30%, respectively. When the concentration of $CaCl_2$ precursor solution increased from 0.8 to 1.2 mol/L, the WPG had the highest rate of change, but the WPG of CI, CI-HT-1.5, and CI-HT-3 decreased successively. The possible reason is that water absorption of wood decreases with increasing heat treatment time, making it difficult to provide stable attachment sites for water molecules and $CaCO_3$ crystallization [31–33].

When the impregnating solution concentration increased from 1.2 to 1.6 mol/L, the WPG of CI, CI-HT-1.5, and CI-HT-3 only increased by 1.05%, 1.00%, and 2.03%. The main reason for the lower increase in WPG is that the high concentration of the impregnating solution led to the formation of $CaCO_3$, which is prone to agglomeration. However, adherence to the wood surface can block some ducts or grain pores, preventing further calcium carbonate production inside the wood. Therefore, as described in the literature, WPG is related to the precursor solution concentration, and the high concentration is not conducive to the formation of $CaCO_3$ inside the wood [34]. Consequently, the impregnating solution concentration in subsequent experiments was preferentially 1.2 mol/L.

3.2 Effects of in-situ Synthesized in $CaCO_3$ on Physical and Mechanical Properties

The equilibrium moisture content (EMC), the surface hardness (HD), the modulus of rupture (MOR), and the modulus of elasticity (MOE) , and the density of the untreated, heat-treated, and $CaCO_3$ modified samples are shown in Figs. 3, 4 and Table 2.

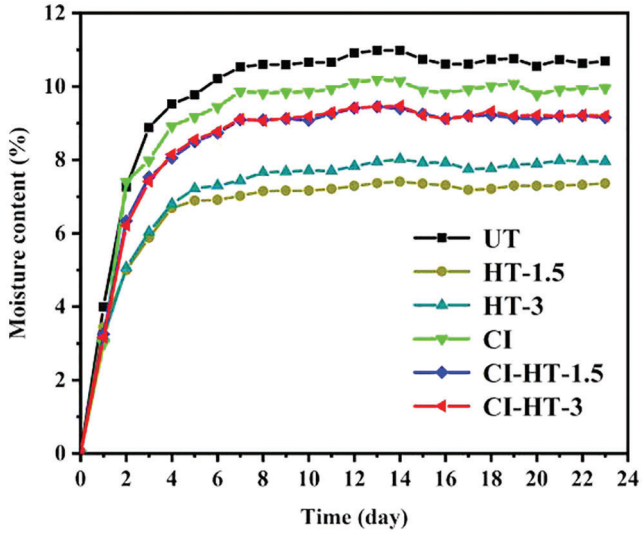

Figure 3: The EMC of the untreated, heat-treated and $CaCO_3$ modified samples

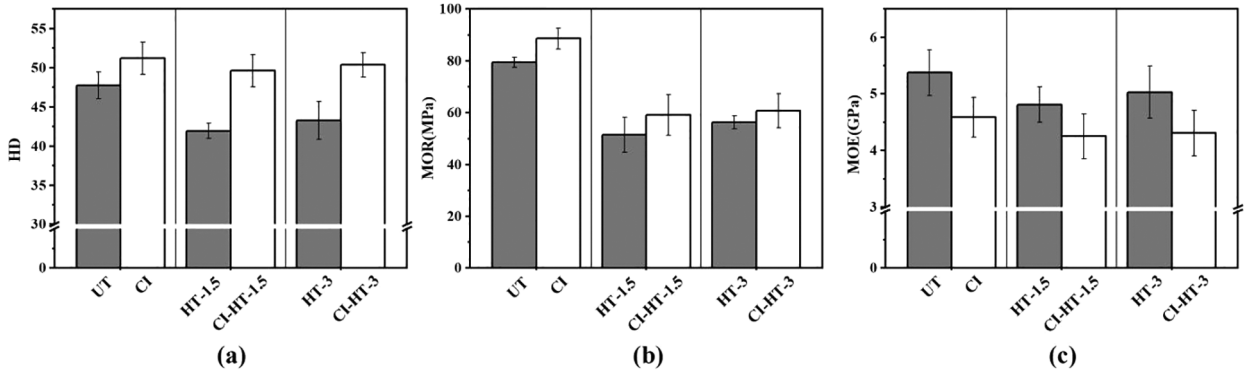

Figure 4: The surface hardness (a), Modulus of rupture (b), and modulus of elasticity (c) of the untreated, heat-treated and $CaCO_3$ modified samples

Table 2: Physical and mechanical properties of the modified wood samples

Groups	Density (kg/m^3)	Surface hardness Shore D (HD)	Modulus of rupture (MPa)	Modulus of elasticity (MPa)
UT	412.03 ± 14.50	47.75 ± 1.72	79.41 ± 1.97	5376.48 ± 402.13
CI	457.90 ± 17.13	51.23 ± 2.05**	88.63 ± 3.96*	4591.98 ± 349.53**
HT-1.5	410.88 ± 6.10	41.95 ± 0.99	51.56 ± 6.76	4811.84 ± 314.386
CI-HT-1.5	443.11 ± 11.91	49.65 ± 2.05**	59.11 ± 7.82	4251.69 ± 393.65**

(Continued)

Table 2 (continued)

Groups	Density (kg/m^3)	Surface hardness Shore D (HD)	Modulus of rupture (MPa)	Modulus of elasticity (MPa)
HT-3	392.07 ± 13.50	43.30 ± 2.41	56.13 ± 4.37	5030.54 ± 458.46
CI-HT-3	418.08 ± 12.27	50.38 ± 1.57**	61.12 ± 7.79	4308.98 ± 405.58**

Note: The data are standard values and standard deviations. Comparison of poplar wood samples before and after *in-situ* synthesis of $CaCO_3$. Asterisks denote significant difference, $P^* \leq 0.05$; $P^{**} \leq 0.01$.

The EMC of the HT-1.5 and HT-3 were reduced, as shown in Fig. 3. This is due to the fact that poplar wood undergoes a HT process in which the hemicellulose is subjected to pyrolysis and hydrolysis reactions, reducing the number of hydrophilic groups such as free hydroxyl groups [35]. In addition, the crystallinity of the cellulose and the size of the crystals in the heat-treated wood increase due to the heat, which also reduces its hygroscopicity, resulting in a lower equilibrium moisture content [35]. Compared with HT-1.5 and HT-3, the EMC of CI-HT-1.5 and CI-HT-3 increased slightly. However, they were obviously lower than that of UT. The EMC of CI reduced duo to the mineralization process, CI had the highest increment of the $CaCO_3$. Previous study shown that the $CaCO_3$ deposited in the internal void structure of poplar wood would impede the movement of moisture, thus reducing the hygroscopicity [36].

Table 2 shows that the increasing rate of density for each group is consistent with the results of the WPG. The density of the heat-treated samples decreased due to the degradation of cell wall components during the HT process [37]. The mechanical properties of UT are similar to the literature, while the MOR and MOE of heat-treated wood is lower [35]. Compared to UT, the mechanical properties of the HT-1.5 and HT-3 decreased. The HD value of HT-1.5 and HT-3 were 41.95 and 43.30, which were 12.15% and 9.32% lower than that of UT. Besides, the MOR and MOE of the HT-3 were 29.32% and 6.43% lower than in the UT samples.

Fig. 4 indicates the HD and MOR of untreated and heat-treated samples were enhanced by *in-situ* filling with $CaCO_3$. Although the impregnation process may negatively affect wood mechanical properties, the optimization of the wood structure by the filling effect of $CaCO_3$ compensated for this loss, except for stiffness. In other words, the *in-situ* synthesis of $CaCO_3$ filled some of the voids in wood cell walls and cell lumina [38].

The HD values of CI, CI-HT-1.5, and CI-HT-3 were 51.23, 49.65, and 50.38, respectively, improved by 7.29%, 18.36%, and 16.35%, respectively, all with highly significant differences from the UT ($P < 0.01$). The *in-situ* synthesis of $CaCO_3$ significantly improved the bending strength of CI ($P > 0.05$). The bending strength of CI-HT-1.5, and CI-HT-3 improved to same extent. The MOR values were 59.11 and 61.12 MPa. The decrease in MOE of CI, CI-HT-1.5 and CI-HT-3 is found in Table 2, compared with UT, HT-1.5, HT-3, all with highly significant differences ($P < 0.01$). It was indicated that $CaCO_3$ crystals could effectively enhance the cell wall of heat-treated wood and improve its surface hardness [34], and improve the bending strength accordingly.

Cluster analysis was done based on values of the HD, MOR, and MOE values; the dendrogram of those clusters is shown in Fig. 5. The dendrogram of HCA for various samples regarding HD shows two main clusters; the CI and CI-HT-3 were classified into the first group, which also contains UT and CI-HT-1.5. The HT-1.5 and HT-3 were classified into the second group, further proving that the HD of the heat-treated wood was improved by the *in-situ* filling with $CaCO_3$.

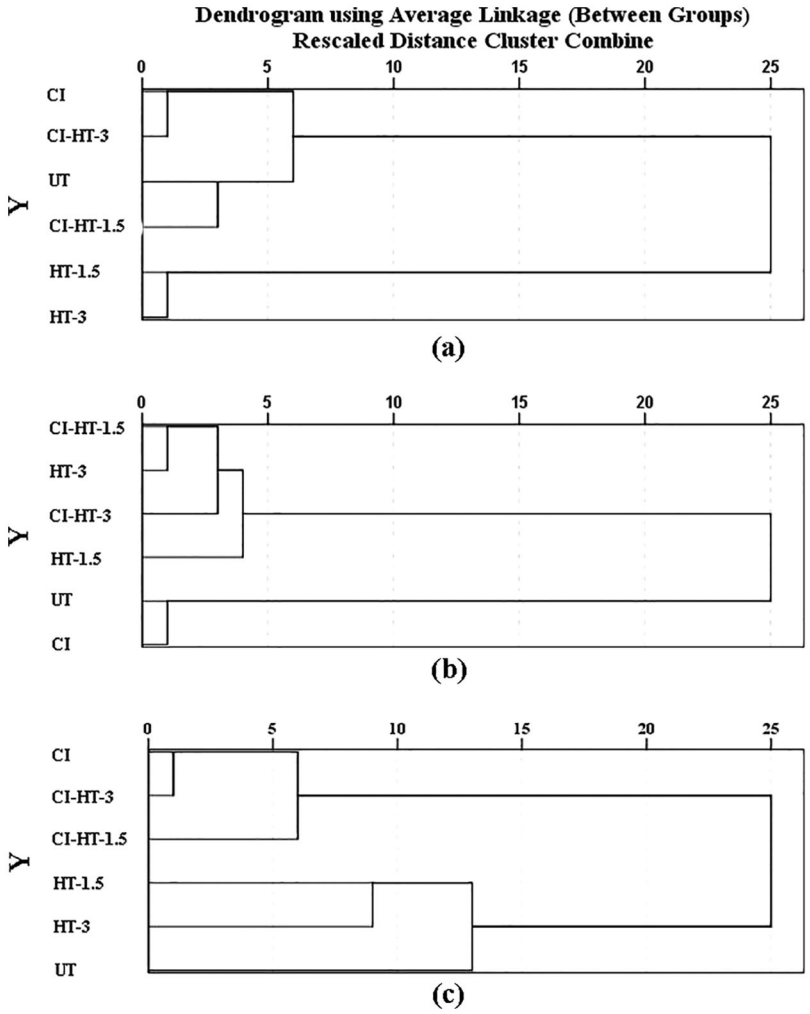

Figure 5: Hierarchical cluster analysis (HCA) of HD (a), MOR (b), and MOE (c) based on different variables

Note: The horizontal axis shows the distances of clusters, and the vertical axis shows treatment groups.

For MOR, the dendrogram of HCA was grouped into two blocks, CI-HT-1.5, HT-3, CI-HT-1.5, and HT-1.5 were classified into the first group. Regarding the MOE dendrogram, the CI, CI-HT-1.5, and CI-HT-3 were classified into the same group, and UT, HT-200–1.5, and HT-200–3 belonged to another group. It also verified that $CaCO_3$ *in-situ* synthesized improves the deficiency of surface hardness and mechanical properties of the heat-treated wood.

3.3 Effects of in-situ Synthesized in $CaCO_3$ on Thermal Stability

Fig. 6 represents the TG/DTG curves of the $CaCO_3$ modified samples. The TG curves of HT-1.5 and HT-3 samples were assembled with that of UT, so as stated in the literature, high-temperature HT cannot significantly affect the pyrolytic properties of the wood [39]. It worth noting that the thermal stability of poplar wood was enhanced after the modification of *in-situ* filling with $CaCO_3$.

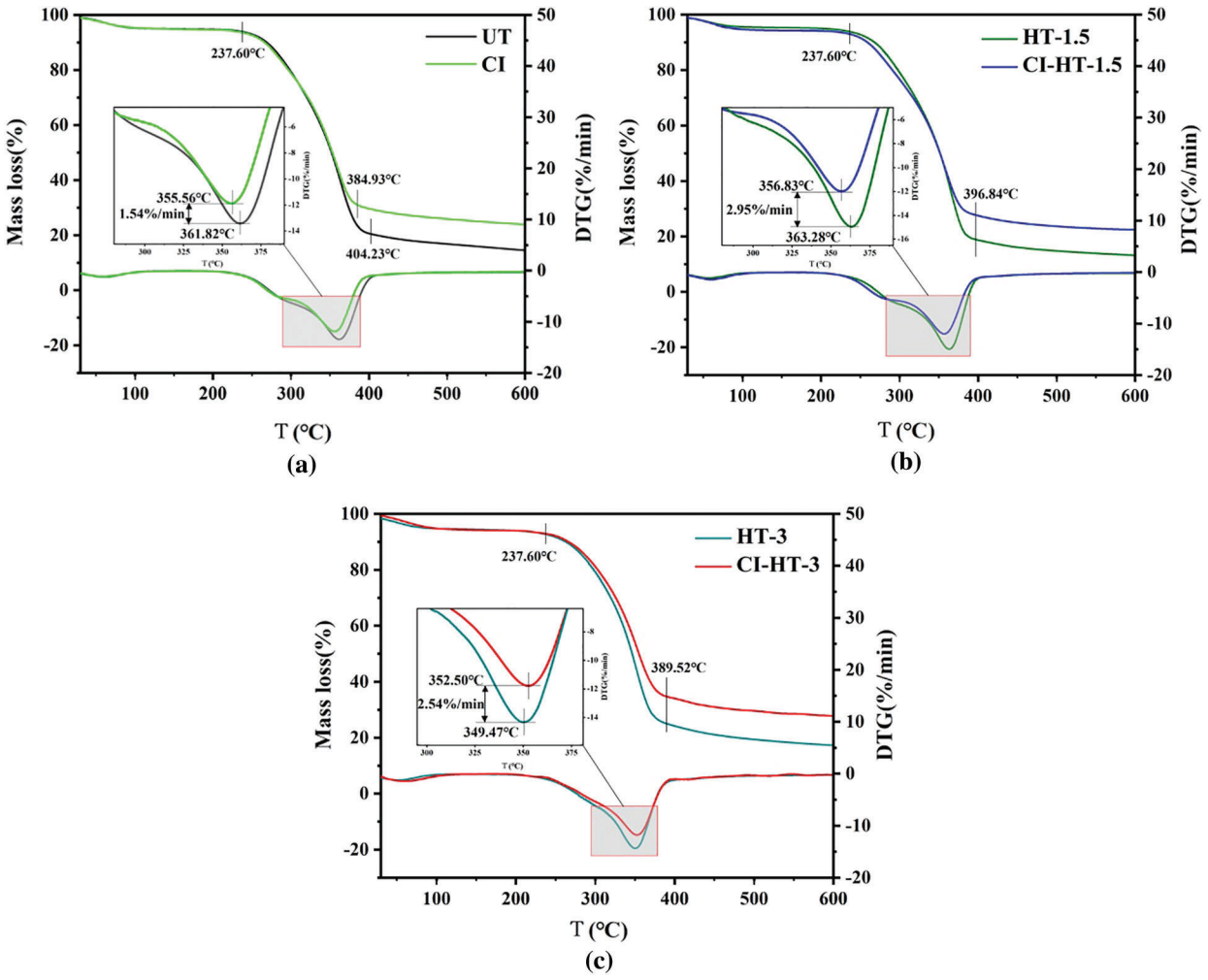

Figure 6: TG/DTG curves of the untreated, heat-treated and $CaCO_3$ modified wood

The thermal behavior of poplar wood was divided into four stages (Fig. 6) [25]. The initial stage is the drying stage, which is attributed to the evaporation and desorption of residual water in the sample with the temperature below 120°C–150°C. Afterwards the unstable components of the wood, such as hemicellulose, decompose in small amounts. The cellulose and hemicellulose pyrolysis mostly transpired in the third stage with the temperature from 237.60°C to 404.23°C. The weight loss of the wood at the third stage reached 73.24%. The temperature of 361.82°C was correspondent to the maximum rate of pyrolysis. In the last stage, the temperature exceeds 404.23°C, and the wood mass stabilizes, mainly due to the decomposition of char products [40].

Compared to UT, the char residue of HT-1.5 decreased by 1.01%, and the maximum weight loss rate increased by 11.33%; there was no distinct difference in the temperature corresponding to their maximum weight loss rate. For the HT-3, the char residue increased by 3.11%, and the temperature corresponding to the maximum weight loss decreased by 12.4°C, indicating that high-temperature and long duration HT may negatively influence wood thermal stability. The DTG curves of HT-3/CI-HT-3 in the second stage were plateau, and no shoulder peak was generated (Fig. 6c). This phenomenon is relevant to hemicellulose decomposition, of which the rate of degradation increases with the prolonged HT time [40,41].

Because of the *in-situ* filling with $CaCO_3$, the char residue of CI, CI-HT-1.5, and CI-HT-3 increased by 9.09%, 9.31%, and 9.69%, respectively. Furthermore, the maximum weight loss rate decreased by 11.48%, 19.80%, and 17.79%, respectively. It could be explained that the *in-situ* synthesis of $CaCO_3$ can effectively improve the thermal stability of heat-treated poplar wood, because of the filling of the $CaCO_3$.

3.4 FTIR Analysis

Fig. 7 demonstrates the FTIR spectrum of the $CaCO_3$ modified wood. The HT changes the wood structure and degrades cell wall compounds and wood extractives [42]. Besides, there is an insignificant difference between the chemical composition of the HT-1.5 and HT-3 wood (Figs. 7b and 7c) [43]. Table 3 lists the absorbance ratios of the modified poplar wood samples.

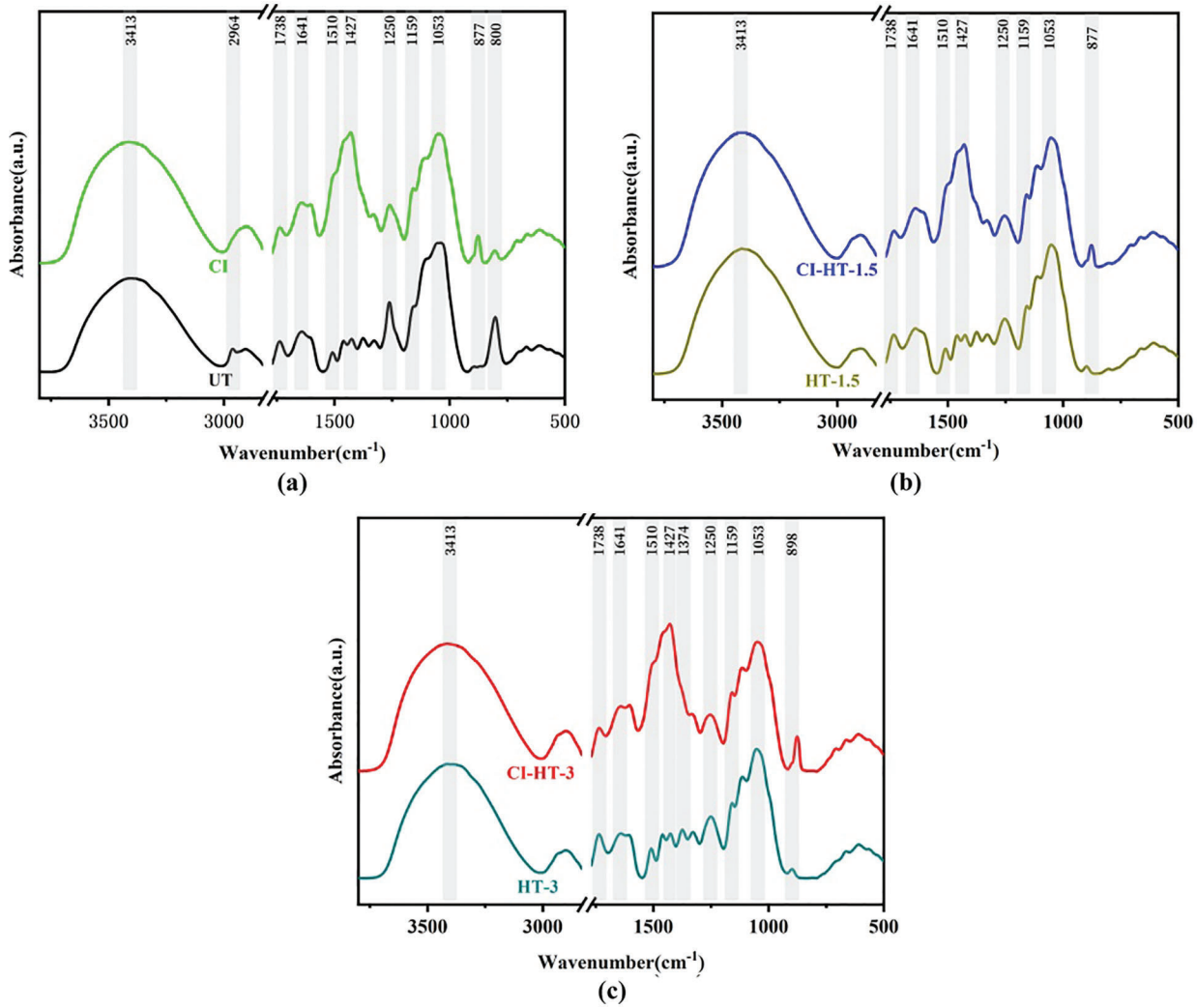

Figure 7: The FTIR spectrum of the UT/CI (a), HT-1.5/CI-HT-1.5 (b), and HT-3/CI-HT-3 (c) samples

Table 3: Absorbance ratios of the modified poplar wood samples

Groups	I1510/I1374	I1510/I1159	I898/I1427	I898/I1510	I1053/I1427
UT	0.600625	0.317208	0.182502	0.302797	3.640574
CI	1.299405	1.112058	0.073304	0.112280	0.972264
HT-1.5	0.611188	0.394671	0.176336	0.265505	2.896756
CI-HT-1.5	1.251924	1.045685	0.067857	0.106642	1.041371
HT-3	0.611188	0.394671	0.253785	0.382119	2.896756
CI-HT-3	1.314151	1.300854	0.073793	0.104280	0.867776

Wood is mainly composed of cellulose, hemicellulose, and lignin [44]. The peak height ratio of the characteristic absorption peaks of lignin to cellulose, hemicellulose and carbohydrates can be used to determine the relative lignin content [45]. The characteristic peak at 1510 cm^{-1} is the aromatic skeleton of C=C vibration, which, like 1427 cm^{-1}, is the characteristic peak representing lignin in the cell wall [46–48]. Moreover, a spectral peak at 1053 cm^{-1} corresponds to C-O deformation in cellulose 0. I1053/I1427 reflects the relative content of lignin, and it can be seen from Table 3 that its relative value does not change with increasing heat treatment duration [49]. The peak at 1374 cm^{-1} depicts the presence of C-H deformation, aliphatic C-H stretching in phenol and methyl group of cellulose and hemicellulose [50,51]. And the peak at 1159 cm^{-1} represents C-O-C symmetric stretching in pyranose rings, C=O stretching in aliphatic groups of cellulose and hemicellulose [51,52]. I1510/I1374 andI1510/I1159 reflect the relative content of holocellulose, there were no changes between HT-1.5 and HT-3 [49]. The peak at 898 cm^{-1} is attributed to C-H stretching out of the plane of the aromatic ring of glucose in cellulose 0. I898/I1427 and I898/I1510 reflect the relative content of cellulose, increased with the extension of HT duration [49]. It follows that the constant wood total cellulose and the gradual increase in cellulose indicate the degradation of hemicellulose, which is similar to the results reported in the literature [53,54]. The thermal degradation becomes more intense as the treatment time increases, and the hemicellulose is interspersed between the microfibril and lignin, which acts like a bond, thus causing a reduction in the mechanical strength of the thermally modified material [55].

Fig. 7 shows a strong peak at 1738 cm^{-1}, mainly caused by the vibration of -C=O- [46]. However, this vibration is weakened after the *in-situ* synthesis of the sample by $CaCO_3$, which is perhaps relevant to the acetic acid produced by the hydroxyl group in part of the sugar group in hemicellulose hydrolyzed with the acetyl group. During the modification process, the acetic acid reacts with the alkaline impregnating solution of the modified samples, causing partial hydrolysis of the acetyl group consisting of -CH_3 and C=O. Consequently, the intensity of the peak of the acetyl group in the infrared spectrogram of the modified wood samples is weakened [30,56]. Furthermore, the characteristic peaks of calcium carbonate at 1427 and 877 cm^{-1} were not detected in the unmodified wood and thermally modified wood samples. The peak at 877 cm^{-1} assigned to CO_3^{2-} [57] indicates that $CaCO_3$ was deposited uniformly in the wood cell lumen.

3.5 XRD and SEM Analysis

Table 4 shows the changes in relative crystallinity. Wood cellulose showed characteristic reflections at 2θ of 16.0° (101) and 22.0° (002). The crystallinity of the heat-treated wood increased significantly with increasing HT duration, which is probably because of the of amorphous cellulose degradation [57]. Besides, pseudocrystalline regions are formed in the amorphous regions due to the re-formation of crystalline degradation products of the hemicellulose and lignin during the steam and heat process [58];

In addition, heat-induced stress release within the wood may also cause the increase in pseudo crystallinity [59,60]. Wood properties are highly dependent on the chemical compositions, the orientation of cellulose microfibrils, the molecular interactions of the cell wall polymer assembly, and changes in crystallinity [59,61]. The crystallinity of the CI, CI-HT-1.5, and CI-HT-3 samples slightly decreased after the *in-situ* synthesized $CaCO_3$. The reasons are as follows: on the one hand, the alkaline Na_2CO_3 solution degrades some of the hemicellulose and lignin, this leads to the enlargement of the void size of the amorphous region in the cell wall. The increase in the area of the amorphous region leads to a decrease in crystallinity; on the other hand, the solution can cause cellulose to swell and enter the amorphous zone, which leads to greater spacing between cellulose molecular chains, making crystallinity of mineralized samples reducing [62].

Table 4: Changes in relative crystallinity of the modified poplar wood samples

Group	I_{am}	I_{002}	Relative crystallinity
UT	1850.7	3284.5	43.65%
CI	694.3	1195.0	41.90%
HT-1.5	1399.8	2584.3	45.83%
CI-HT-1.5	679.7	1165.3	41.67%
HT-3	1654.5	3412.1	51.51%
CI-HT-3	623.3	1129.7	44.83%

Note: The peak located near $2\theta = 18°$ represents the scattering intensity I_{am} of the diffraction angle of the amorphous region; the peak located near $2\theta = 22°$ indicates that maximum intensity I_{002} of the diffraction angle of the crystal region.

The crystal structure and physical phase of the untreated and $CaCO_3$ modified wood samples were determined and analyzed by XRD, as shown in Fig. 8. Compared with UT, the intensity of these two peaks decreased significantly in the treated samples of HT-1.5, while there was no significant change in the ones of HT-3. There were no other characteristic diffraction peaks observed in Fig. 8, indicating the absence of other impurities in the test samples. In addition, the sufficient crystallinity of the $CaCO_3$ was synthesized in the modified samples.

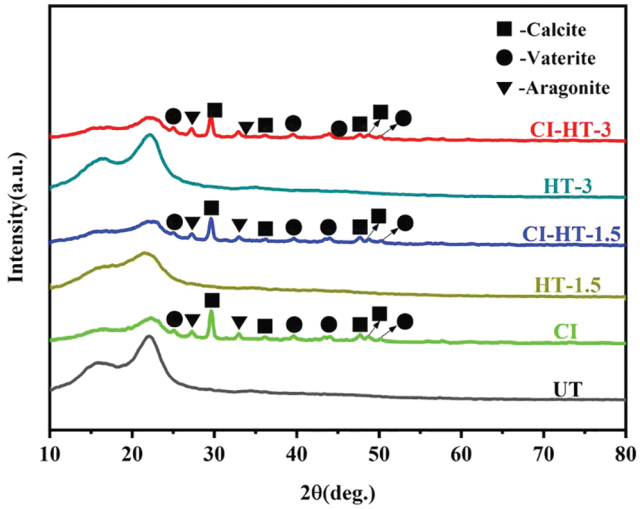

Figure 8: XRD patterns of the modified wood

The diffraction peaks at 2θ = 25.1°, 39.6°, 44.0°, and 50.0° corresponded to the (110), (205), (300), and (118) planes of $CaCO_3$, respectively, which could be indexed to the vaterite (JCPDS 33-0268); The peaks at 2θ = 27.3° and 33.0° corresponded to the (021) and (012) planes of $CaCO_3$, respectively, which could be indexed to the aragonite (JCPDS 41-1475); The peaks at 2θ = 29.6°, 36.1°, 47.7°, and 48.7° corresponded to the (104), (110), (018) and (116) planes of $CaCO_3$, respectively, which could be indexed to the well-crystallized calcite (JCPDS 05-0586). Furthermore, the $CaCO_3$ crystal types in the samples of CI, CI-HT-1.5, and CI-HT-3 were approximately the same. In another word, no matter if the samples were heat-treated or not, wherein the $CaCO_3$ crystal is mainly in the form of calcite.

3.6 SEM Analysis and Characterization

The morphologies and microstructures of the $CaCO_3$ modified wood were investigated by SEM. Figs. 9a–9c show that a layer of $CaCO_3$ particles covered the surface of CI wood. While the pore size of the $CaCO_3$ distribution was narrower, the diameter particles were larger and rhombic polyhedral in the heat-treated wood.

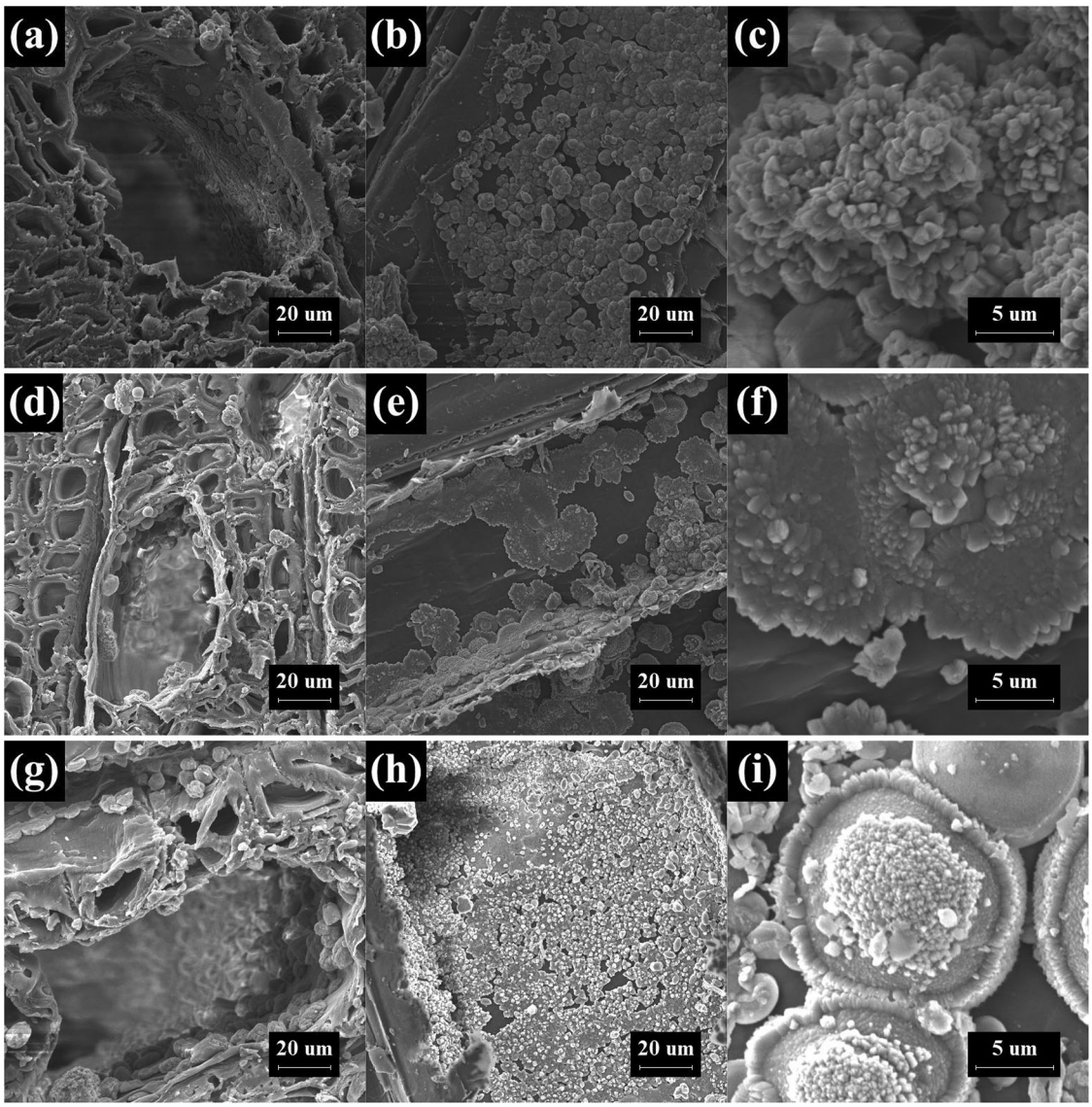

Figure 9: SEM images of CI (a–c), CI-HT-1.5 (d–f), and CI-HT-3 (g–i), wherein a, d, g are cross section (×1.0 k), b, e, h are tangential section (×1.0 k), c, f, i are radial section (×6.0 k)

Figs. 9d and 9e are SEM images of CI-HT-1.5, the $CaCO_3$ particles were evenly distributed in the cell cavity of the wood fiber, and the $CaCO_3$ was regularly arranged. Furthermore, $CaCO_3$ particles were distributed in patches on the walls of the vessels, and there was also a distribution of granular $CaCO_3$ in the ray cells consistent with cross-sectional observations. The evenly distributed lumps of $CaCO_3$ can be seen on the inner the duct wall and the grain pore area on the wood rays. On top of that, the grain pores were incompletely covered by the $CaCO_3$ particles. This finding indicates that the $CaCl_2$ and Na_2CO_3 solutions can flow in the wood vessel and ray cells during the impregnation process, resulting in a more efficient deposition modification.

The SEM images of CI-HT-3 were shown in Figs. 9g and 9i. There were well-proportioned $CaCO_3$ particles generated in inner wall of the vessels and the inner wall of the cell wall. Some particles embedded in the interior of the cell wall and covered by wood fibers, which was due to the reaction of the precursor solution penetrated inside the cell wall to produce $CaCO_3$. It can be found that $CaCO_3$ particles were distributed in patches on the inner wall of the vessels, interestingly, with some spreading outward with the nucleus as the center. In the meantime, the primary nuclei were anchored into the cell wall region where the larger particles would grow at the expense of the smaller ones by the so-called "Ostwald ripening process" [63]. As the result, the $CaCO_3$ particles are mostly spherical or small clusters in the radial section, as shown in Figs. 9h and 9i. In this growth process, some constant precipitation of very fine primary nuclei of $CaCO_3$ occurred on the inner wall of the duct and the cell wall where the Na_2CO_3 solution was just injected.

4 Conclusions

The effects of the *in-situ* reinforcement of $CaCO_3$ on the weight percent gain and mechanical properties, as well as the thermal stability of the heat-treated poplar wood were investigated. The conclusions were drawn as follows:

The filling amount of $CaCO_3$ in heat-treated wood increased with the increasing concentration of impregnating solution, the *in-situ* synthesis amount of $CaCO_3$ can be initially regulated by adjusting the ratio of $CaCl_2$ to Na_2CO_3 solution. Moreover, the HT process played a central role in the filling amount of $CaCO_3$ in wood. Furthermore, the incorporation of the $CaCO_3$ retarded the thermal decomposition of wood, resulting in improved thermal stability.

After the HT, the wood's mechanical properties decreased due to the degradation of substrates. The optimization of the wood structure by the filling effect of $CaCO_3$ improved the HD and MOR of the heat-treated wood and compensated for this loss to some extent. The specific material combination of heat-treated plantation wood and *in-situ* synthesis $CaCO_3$ results in a composite material that has the potential to be used as furniture or construction materials. As a result, the application of *in-situ* synthesis $CaCO_3$ could lead to improved mechanical properties and thermal stability of the heat-treated wood. This study provides a new method to extend the utilization of plantation wood. Future research will be focused on the controlling the $CaCO_3$ formation, as well as the fire-proofing improvement of this mineralization process.

Funding Statement: This research was funded by "Natural Science Foundation of Anhui Province, Grant No. 2008085QC130".

Conflicts of Interest: The authors declare that they have no conflicts of interest to report regarding the present study.

References

1. Wang, D. W., Shen, W. X. (2022). The calculation and analysis of carbon storage and carbon sequestration potential of the main artificial arboreal forest in China. *Journal of Nanjing Forestry University (Natural Sciences Edition),* 1–10. DOI 10.12302/j.issn.1000-2006.202109014.

2. Chu, D. M., Mu, J., Avramidis, S., Rahimi, S., Liu, S. Q. et al. (2019). Functionalized surface layer on poplar wood fabricated by fire retardant and thermal densification. Part 1: Compression recovery and flammability. *Forests, 10(11),* 982.
3. Sandberg, D., Kutnar, A., Mantanis, G. (2017). Wood modification technologies-A review. *iForest-Biogeosciences and Forestry, 10(6),* 895–908.
4. Fuchs, W. (1928). Zur kenntnis des genuinen lignins, I.: Die acetylierung des fichtenholzes. *Berichte der Deutschen Chemischen Gesellschaft (A and B Series), 61(5),* 948–951.
5. Chai, Y. B. (2015). *Research on the process and mechanism of wood acetylation (Ph.D. Thesis)*. Chinese Academy of Forestry, China.
6. Gu, L. B. (2012). Current status and application prospects of wood modification. *Chinese Journal of Wood Science and Technology, 26(3),* 1–6.
7. Gu, L. B., Ding, T., Jiang, N. (2019). Development of wood heat treatment research and industrialization. *Journal of Forestry Engineering, 4(4),* 1–11. DOI 10.13360/j.issn.2096-1359.2019.04.001.
8. Chu, D. M., Mu, J., Avramidis, S., Rahimi, S., Lai, Z. Y. et al. (2020). Effect of heat treatment on bonding performance of poplar via an insight into dynamic wettability and surface strength transition from outer to inner layers. *Holzforschung, 74(8),* 777–787.
9. Rahimi, S., Singh, K., DeVallance, D. (2019). Effect of different hydrothermal treatments (steam and hot compressed water) on physical properties and drying behavior of yellow-poplar (*Liriodendron tulipifera*). *Forest Products Journal, 69(1),* 42–52.
10. Xu, K., Li, J. X., Li, X. J., Wu, Y. Q. (2015). Effect of heat treatment on dimensional stability of phenolic resin impregnated poplar wood. *Journal of Beijing Forestry University, 37(9),* 70–77.
11. Phuong, L. X., Shida, S., Saito, Y. (2007). Effects of heat treatment on brittleness of styrax tonkinensis wood. *Journal of Wood Science, 53(3),* 181–186.
12. Kol, H. S., Sefil, Y. (2011). The thermal conductivity of fir and beech wood heat treated at 170°C, 180°C, 190°C, 200°C, and 212°C. *Journal of Applied Polymer Science, 121(4),* 2473–2480.
13. Yang, S., Fu, Y. J., Yan, T. T., Chen, Y. (2021). Effect of high temperature heat-treatment on the chemical properties of *Swietenia macrophylla*. *Journal of Forestry Engineering, 6(2),* 120–125.
14. Dong, H. J., Bahmani, M., Rahimi, S., Humar, M. (2020). Influence of copper and biopolymer/Saqez resin on the properties of poplar wood. *Forests, 11(6),* 667.
15. Wang, G., Chen, X. Y., Huang, R., Zhang, L. (2002). Nano-$CaCO_3$/polypropylene composites made with ultra-high-speed mixer. *Journal of Materials Science Letters, 21(13),* 985–986.
16. Huang, L. L., Yao, X. L., Huang, Y. T., Wang, Q. S. (2018). The preparation of $CaCO_3$/wood composites using a chemical precipitation method and its flame-retardant and mechanically beneficial properties. *BioResources*, *13(3),* 6694–6706.
17. Merk, V., Chanana, M., Keplinger, T., Gaan, S., Burgert, I. (2015). Hybrid wood materials with improved fire retardance by bio-inspired mineralisation on the nano- and submicron level. *Green Chemistry, 17(3),* 1423–1428.
18. Rožle, R., Andreja, P., Davor, K., Miha, H., Andrijana, S. Š. (2022). Combining mineralisation and thermal modification to improve the fungal durability of selected wood species. *Journal of Cleaner Production, 351,* 131530.
19. Lin, Y. X., Gao, C., Chen, M. (2009). Thermomechanical properties and tribological behaviour of $CaCO_3$ whisker-reinforced polyetheretherketone composites. *Proceedings of the Institution of Mechanical Engineers, Part J: Journal of Engineering Tribology, 223(7),* 1013–1018.
20. Chen, L., Xu, W., Chen, C. H., Tang, X. L. (2018). The comparative analysis of the lnorganic modification and performance of the fast growing poplar wood for furniture. *Furniture, 39(2),* 7–10.
21. Tao, X., Chen, L., Xu, W., Chen, C. H., Tang, X. L. (2019). Study on mechanical properties of Nano-TiO_2 impregnated modified poplar wood. *Forestry and Grassland Machinery, 30(1),* 21–23+29.
22. Tao, X., Xu, W., Mao, W. G., Mao, Z. N., Chen, C. H. et al. (2019). Application of modified poplar wood in furnishing products. *Forestry Machinery & Woodworking Equipment, 47(4),* 37–41.

23. Duan, J. T., Zhang, X. L., Wang, Z., Li, J., Li, S. G. et al. (2021). . Effects of inorganic fillers on properties of wood flour/high density polyethylene composites. *Packaging Engineering, 42(3),* 62–68.
24. Li, S. Z., Fu, W. Q., Feng, C. L. (2018). Research progress in environmental exposure, behavior and toxic effect of organophosphorus flame retardants. *Environmental Engineering, 36(9),* 180–184+35.
25. Hu, Y. C. (2006). *Char forming and smoke suppression function of zinc borateand ammonium polyphosphate on wood during combustion (Ph.D. Thesis)*. Central South University of Forestry and Technology, China.
26. Chu, D. M., Mu, J., Zhang, L., Li, Y. S. (2017). Promotion effect of NP fire retardant pre-treatment on heat-treated poplar wood. Part 2: Hygroscopicity, leaching resistance, andthermalstability. *Holzforschung, 71(3),* 217–223.
27. GB/T 17657-2013 (2013). Test methods of evaluating the properties of wood-based panels and surface decorated wood-based panels. Chinese National Committee for Standardization.
28. Guo, F., Huang, R. F., Lu, J. X., Chen, Z. J., Cao, Y. J. (2014). Evaluating the effect of heat treating temperature and duration on selected wood properties using comprehensive cluster analysis. *Journal of Wood Science*, *60(4),* 255–262.
29. Segal, L., Creely, J. J., Martin, A. E., Conrad, C. M. (1959). An empirical method for estimating the degree of crystallinity of native cellulose using the X-ray diffractometer. *Textile Research Journal, 29(10),* 786–794.
30. Shi, J. J., Chen, H., Ye, J. Y., Zhang, Y. T., Wu, Z. H. et al. (2022). Properties of poplar veneer and plywood modified by *in-situ* synthesis of $CaCO_3$. *Journal of Forestry Engineering, 7(2),* 43–51.
31. Yan, M. H. (2021). *Wood properties and dynamic moisture sorption of high-temperature thermally treated larch gmelinii* (*Master's Thesis*). Northeast Forestry University, China.
32. Wu, M. H., Zhao, C. P., Cai, J. B., Jin, J. W., Sun, Z. B. (2020). Effects of impregnation and heat-treatment on microstructure and dimensional stability of poplar. *Journal of Anhui Agricultural University, 47(5),* 738–743.
33. Gao, X., Zhou, F., Zhou, Y. D. (2019). Sorption isotherms characteristics of high temperature heat-treated wood. *Scientia Silvae Sinicae, 55(7),* 119–127.
34. Huang, Y. T. (2016). *Preparation of $CaCO_3$/wood composites its performance research (Master's Thesis)*. Anhui Agricultural University, China.
35. Hao, D. E. (2008). *Study on super temperature heat treated poluar wood* (*Master's Thesis*). Nanjing Forestry University, China.
36. Wang, C. Y., Liu, C. Y., Li, J. (2010). Preparation of hydrophobic $CaCO_3$-wood composite *in situ*. *Advanced Materials Research, 113–116,* 1712–1715.
37. Zhou, Y. Q., Xue, Z. Q., Huang, Q. T., Yao, B., Wang, X. H. (2020). Physical and mechanical properties of *Aucoumea klaineana* wood after vacuum heat treatment for furniture components. *Journal of Forestry Engineering, 5(4),* 73–78. DOI 10.13360/j.issn.2096-1359.201907014.
38. Li, P., Wu, Y. Q., Lv, J. X., Yuan, G. M., Zhuo, Y. F. (2021). Effect of biomimetic respiration method on the lmpregnation effect of silicate modified Chinese fir by XPS and FTIR analysis. *Spectroscopy and Spectral Analysis, 41(5),* 1430–1435.
39. Todaro, L., Rita, A., Cetera, P., D'Auriab, M. (2015). Thermal treatment modifies the calorific value and ash content in some wood species. *Fuel, 140,* 1–3.
40. Hua, C. P., Liu, F., Dong, P. W., Peng, M. (2020). Wood thermogravimetric test and dynamic analysis. *Fire Science and Technology, 39(6),* 757–760.
41. Wang, Z. (2017). *Study on properties and mechanism of larch wood modified by vacuum heat treatment (Ph.D. Thesis)*. The Chinese Academy of Forestry Science, China.
42. Nuopponen, M., Vuorinen, T., Jämsä, S., Viitaniemi, P. (2003). The effects of a heat treatment on the behaviour of extractives in softwood studied by FTIR spectroscopic methods. *Wood Science and Technology, 37(2),* 109–115.
43. Esteves, B., Marques, A. V., Domingos, I., Pereira, H. (2013). Chemical changes of heat treated pine and eucalypt wood monitored by FTIR. *Maderas. Ciencia y Tecnología, 15(2),* 245–258.
44. Asante, B., Ye, H. Z., Nopens, M., Schmidt, G., Krause, A. (2022). Influence of wood moisture content on the hardened state properties of geopolymer wood composites. *Composites Part A: Applied Science and Manufacturing, 152,* 106680.

45. Ding, P., Peng, W. W., Li, T. (2017). Rapid determination of physical and chemical properties of two kinds of solid floor woods with XRD and FTIR approaches. *Spectroscopy and Spectral Analysis, 2(5),* 25–30.
46. Chen, H. L., Ferrari, C., Angiuli, M., Yao, J., Raspi, C. et al. (2010). Qualitative and quantitative analysis of wood samples by Fourier transform infrared spectroscopy and multivariate analysis. *Carbohydrate Polymers, 82(3),* 772–778.
47. Ishimaru, K., Hata, T., Bronsveld, P., Meier, D., Imamura, Y. J. (2007). Spectroscopic analysis of carbonization behavior of wood, cellulose and lignin. *Journal of Materials Science, 42(1),* 122–129.
48. Özgenç, Ö., Durmaz, S., Boyaci, I. H., Eksi-Kocak, H. (2017). Determination of chemical changes in heat-treated wood using ATR-FTIR and FT Raman spectrometry. *Spectrochimica Acta Part A: Molecular and Biomolecular Spectroscopy, 171,* 395–400.
49. Qi, W. Y., Liu, C., Chen, J. M., Wu, X. L., Yang, M. Y. et al. (2021). Effect of N_2 heat treatment on main properties of pinus sylvestris var.mongolica wood. *Journal of Northwest Forestry University, 36(5),* 161–167.
50. Colom, X., Carrillo, F., Nogués, F., Garriga, P. (2003). Structural analysis of photodegraded wood by means of FTIR spectroscopy. *Polymer Degradation and Stability, 80(3),* 543–549.
51. Sharma, V., Yadav, J., Kumar, R., Tesarova, D., Ekielski, A. et al. (2020). On the rapid and non-destructive approach for wood identification using ATR-FTIR spectroscopy and chemometric methods. *Vibrational Spectroscopy, 110,* 103097.
52. Lehto, J., Louhelainen, J., Huttunen, M., Alén, R. (2017). Spectroscopic analysis of hot-water- and dilute-acid-extracted hardwood and softwood chips. *Spectrochimica Acta Part A: Molecular and Biomolecular Spectroscopy, 184,* 184–190.
53. Traoré, M., Kaal, J., Cortizas, M. A. (2016). Application of FTIR spectroscopy to the characterization of archeological wood. *Spectrochimica Acta. Part A: Molecular and Biomolecular Spectroscopy, 153,* 63–70.
54. Yuan, H. M., Guo, X., Wu, Y. Q., Ma, Q., Xiao, T. (2020). Application of micro-FTIR spectroscopy to study molecular structure of desorbed water in heat-treated wood during moisture desorption process. *Journal of Wood Chemistry and Technology, 40(1),* 33–43.
55. Kojima, E., Yamasaki, M., Imaeda, K., Lee, C. G., Sugimoto, T. Y. et al. (2020). Effects of thermal modification on the mechanical properties of the wood cell wall of soft wood: Behavior of S2 cellulose microfibrils under tensile loading. *Journal of Materials Science, 55(12),* 5038–5047.
56. Qian, C. L. (2020). *Preparation and performance of $CaCl_2$-$NaCO_3$ internal reaction deposition modified poplar* (*Master's Thesis*). Nanjing Forestry University, China.
57. Zhang, B., Xiao, X., Han, Y. J., Zhang, Y. Y., Yu, H. W. (2021). Study on third-step infrared spectroscopy of calcium carbonate. *Inorganic Chemicals Industry, 53(1),* 97–101.
58. Li, L. L. (2018). *Study on preparation and recovery mechanism of thermally compressed Scots pine (Pinus sylvestris L.) (Ph.D. Thesis)*. Inner Mongolia Agricultural University, China.
59. Yin, J. P., Yuan, T. Q., Lu, Y., Song, K. L., Li, H. Y. et al. (2017). Effect of compression combined with steam treatment on the porosity, chemical compositon and cellulose crystalline structure of wood cell walls. *Carbohydrate Polymers, 155,* 163–172.
60. Kiemle, S. N., Zhang, X., Esker, A. R., Toriz, G., Gatenholm, P. et al. (2014). Role of (1,3)(1,4)-β-glucan in cell walls: Interaction with cellulose. *Biomacromolecules, 15(5),* 1727–1736.
61. Wei, L. Q., McDonald, A. G. (2016). A review on grafting of biofibers for biocomposites. *Materials, 9(4),* 303.
62. Zhang, Y. Z. (2021). *Wood mineralization based on transpiration of standing trees* (*Master's Thesis*). Inner Mongolia Agricultural University, China.
63. Sugimoto, T. (1987). Preparation of monodispersed colloidal particles. *Advances in Colloid and Interface Science, 28,* 65–108.